AFFTC-PA-11118

Multipath Propagation for Helicopter-to-Ground MIMO Links

Michael Rice, Michael Jensen

AIR FORCE FLIGHT TEST CENTER
EDWARDS AFB, CA

June 2, 2011

A
F
F
T
C

AIR FORCE FLIGHT TEST CENTER
EDWARDS AIR FORCE BASE, CALIFORNIA
AIR FORCE MATERIEL COMMAND
UNITED STATES AIR FORCE

REPORT DOCUMENTATION PAGE

Form Approved
OMB No. 0704-0188

1. REPORT DATE *(DD-MM-YYYY)*	**2. REPORT TYPE**	**3. DATES COVERED** *(From - To)*
02-06-2011	Technical Brief	June 11 – Nov 11

4. TITLE AND SUBTITLE

Multipath Propagation for Helicopter-to-Ground MIMO Links

5a. CONTRACT NUMBER

5b. GRANT NUMBER

5c. PROGRAM ELEMENT NUMBER

6. AUTHOR(S)

Michael Rice and Michael Jensen

5d. PROJECT NUMBER

5e. TASK NUMBER

5f. WORK UNIT NUMBER

7. PERFORMING ORGANIZATION NAME(S) AND ADDRESS(ES) AND ADDRESS(ES)

Brigham Young University

8. PERFORMING ORGANIZATION REPORT NUMBER

AFFTC-PA-11118

9. SPONSORING / MONITORING AGENCY NAME(S) AND ADDRESS(ES)

Tom Young, EA
AFMC, AFFTC, 412 Test Wing
Edwards AFB, CA 93524

10. SPONSOR/MONITOR'S ACRONYM(S)

N/A

11. SPONSOR/MONITOR'S REPORT NUMBER(S)

12. DISTRIBUTION / AVAILABILITY STATEMENT

Approved for public release A: distribution is unlimited.

13. SUPPLEMENTARY NOTES

CA: Air Force Flight Test Center Edwards AFB CA CC: 012100

14. ABSTRACT

Air-to-ground communication for aeronautical telemetry is often impaired by multipath propagation, particularly when the aircraft is near the flight-line. This paper experimentally studies such a channel using measurements from multiple antennas on a helicopter to multiple receiving antennas on the ground as the helicopter maneuvers on a taxiway near hangars and other buildings at Cairns Army Airfield, Ft. Rucker, AL. Analysis of the results reveals delay spreads of the multipath channels between 200 ns and 400 ns, with the longer delay spreads resulting when using a receive antenna with lower gain and higher sidelobe levels such that it that observes richer multipath propagation. The data also shows that on average, diversity signaling from three aircraft-mounted antennas can lead to gains in signal-to-noise ratio of approximately 13 dB, with the gain dependent on the multipath characteristics observed by the ground antenna.

15. SUBJECT TERMS

Aeronautical telemetry; antenna; aircraft antennas; SNR; MIMO links

16. SECURITY CLASSIFICATION OF:			**17. LIMITATION OF ABSTRACT**	**18. NUMBER OF PAGES**	**19a. NAME OF RESPONSIBLE PERSON**
Unclassified					412 TENG/EN (Tech Pubs)
a. REPORT	**b. ABSTRACT**	**c. THIS PAGE**			**19b. TELEPHONE NUMBER** *(include area code)*
Unclassified	Unclassified	Unclassified	None	6	661-277-8615

Multipath Propagation for Helicopter-to-Ground MIMO Links

Michael Rice and Michael Jensen
Brigham Young University
Provo, UT 84602
Email: mdr@byu.edu, jensen@byu.edu

***Abstract*—Air-to-ground communication for aeronautical telemetry is often impaired by multipath propagation, particularly when the aircraft is near the flight-line. This paper experimentally studies such a channel using measurements from multiple antennas on a helicopter to multiple receiving antennas on the ground as the helicopter maneuvers on a taxiway near hangars and other buildings at Cairns Army Airfield, Ft. Rucker, AL. Analysis of the results reveals delay spreads of the multipath channels between 200 ns and 400 ns, with the longer delay spreads resulting when using a receive antenna with lower gain and higher sidelobe levels such that it that observes richer multipath propagation. The data also shows that on average, diversity signaling from three aircraft-mounted antennas can lead to gains in signal-to-noise ratio of approximately 13 dB, with the gain dependent on the multipath characteristics observed by the ground antenna.**

I. Introduction

In aeronautical telemetering, measurements obtained on an airborne test article are radioed to a ground station for monitoring by flight test engineers. As airborne systems become more sophisticated, the number of measurements increases, requiring higher communication data rates. These higher data rates increase the bandwidth of the modulated carrier used to radio the measurements to the ground. As bandwidth increases, the multipath propagation environment becomes more frequency selective [1] and multipath interference becomes the dominant link impairment.

In its current form, the typical aeronautical telemetry system comprises an airborne transmitter and a ground station equipped with a large tracking antenna. The relatively narrow beamwidth of the ground-based receive antenna tends to attenuate off-boresite reflections in the propagation path for "up and away" flight profiles. However, low-elevation-angle and flight-line scenarios present serious challenges. Prior evaluations of the multipath characteristics of such scenarios include experiments conducted at the Air Force Flight Test Center, Edwards Air Force Base in L- and S-bands [2] and at Pt. Mugu Naval Air Station over the Pacific Ocean in X-band [3]. These experiments provided useful data for low-elevation-angle propagation in the "up and away" scenario at test ranges in the western United States. One shortcoming of these experiments, however, is the absence of flight-line propagation data.

This work was supported by the Test Resource Management Center (TRMC) Test and Evaluation Science and Technology (T&E/S&T) Program through a grant from the Army PEO STRI Contracting Office under contract W900KK-09-C-0016.

In the context of aeronautical telemetry, understanding multipath propagation allows engineers to identify and evaluate the performance of multipath mitigation techniques, which may be broadly categorized as diversity or equalization methods. Diversity techniques have had limited appeal in aeronautical telemetry due to cost – the expense of using more than one (expensive) tracking antenna to realize spatial diversity on the ground and the cost of additional bandwidth required to realize frequency and temporal diversity – and little work has been done to consider the impact of using spatial diversity on the air vehicle. Consequently, equalization techniques have received the most attention [4] – [10]. However, the emphasis in this prior work has been on blind and adaptive techniques, with the reported results presenting a relatively weak case for using such blind and adaptive forms of equalization as a multipath mitigation technique in aeronautical telemetry.

To address these shortcomings, this paper reports the results of channel sounding experiments conducted along the flight-line at the Cairns Army Airfield at Ft. Rucker, AL. The measurements, conducted over a 50 MHz bandwidth at L-band, used multiple transmit antennas on the aircraft and multiple receive antennas on the ground, providing data relevant for analysis of both equalization and spatial diversity mitigation techniques. We show that in this environment, delay spreads of the multipath channels vary from about 200 ns to 400 ns, with the variability strongly dependent on the transmit antenna placement and the receive antenna radiation characteristics. We also show that on average, diversity signaling from multiple aircraft-mounted antennas can lead to gains in signal-to-noise ratio (SNR) of approximately 13 dB, with the gain notably dependent on the multipath characteristics observed by the ground antenna.

II. Experimental Configuration

A. System Description

A block diagram of the experimental configuration is illustrated in Figure 1. The 50 MHz channel sounding signal is periodic with a period of 100 kHz and consists of 501 unmodulated tones with 100 kHz spacing. The resulting channel sounding signal, centered at 1800 MHz (upper L-band), is applied to four different transmit antennas, each with a dedicated 10 W Remec power amplifier backed off to meet

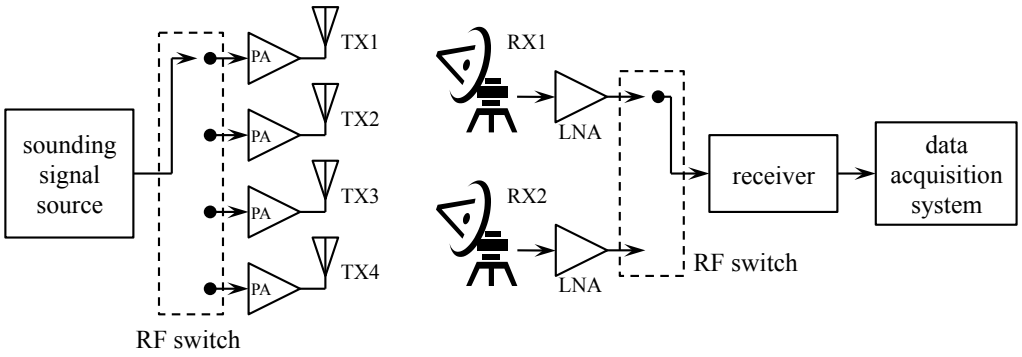

Fig. 1. A block diagram of the channel sounding experiments.

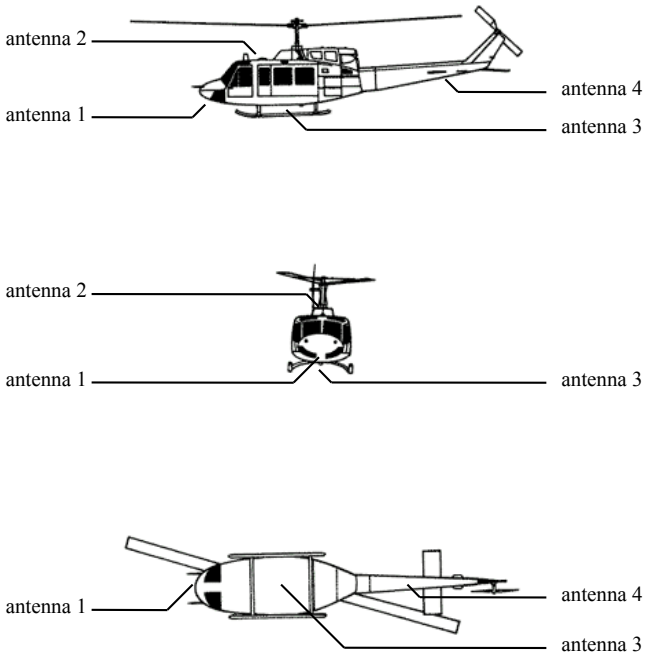

Fig. 2. The UH-1H airborne platform and the transmit antenna locations.

TABLE I
TRANSMIT ANTENNA LOCATIONS

	fuselage station (inches)	waterline (inches)	butt line (inches)
Antenna 1	0	22	0
Antenna 2	85	85	0
Antenna 3	100	10	0
Antenna 4	400	65	0

TABLE II
DESCRIPTION OF THE RECEIVE ANTENNAS.

Antenna	diameter	comments:
RX1	6 ft.	elevation = 60 ft. AGL, tracking performed by conical scan
RX2	4 ft.	elevation = 60 ft. AGL, tracking performed by steering using GPS data downlinked from the UH-1H

spectral occupancy regulations, using a Herley F9140W RF switch. The dwell time for each switch position is 50 μs (5 periods of the channel sounding signal). The transmit antennas are small blade antennas (UB Corp. AO4459) mounted on the fuselage of the UH-1H helicopter platform illustrated in Figure 2. This figure also shows the general placement of the four transmit antennas, with the exact antenna locations listed in Table I.

The ground station (receiver) uses two dish antennas with tracking capability, the details of which are summarized in Table II. The RF outputs from each receive antenna are routed to a single receiver chain through a second switch, with the controlling switch clock synchronized to the transmit switch clock through disciplined rubidium oscillators. The dwell time for each transmit antenna is 250 μs, which accommodates one 50 μs slot for each of the four transmit antennas and one 50 μs blank period used for synchronization during data post-processing. The RF switch output is applied to a Cobham M/A-COM SMR-5550i microwave receiver, and the resulting intermediate frequency (70 MHz) signal is sampled at 200 Msamples/s by a Wideband Systems (DRS2200-144GB-2CHA1) data acquisition system and stored. GPS data is also recorded on the aircraft and is incorporated into the post-processing.

B. Flight Profile

The flight path together with the receive antenna locations are illustrated in Figure 3. The UH-1H flew along the flight path called the "ramp" at an altitude of 15 – 20 feet above ground level (AGL). The receive antennas, shown near the bottom of Figure 3, were elevated to 60 feet AGL using dedicated towers. This arrangement is used at Cairns Army Airfield to allow clearance over the buildings and hangars positioned between the runways (not shown) and the main telemetry receiving center. The "ramp" area presents a particularly troublesome area because typical helicopter altitudes are insufficient to produce line-of-sight (LOS) propagation. The hangars and buildings not only shadow the transmitted signal, but also provide ample opportunity for strong multipath propagation.

Fig. 3. The flight path at Cairns Army Airfield, Ft. Rucker, AL. The UH-1H flight path is the "ramp" area shown. The two receive antennas are located on towers situated at the bottom of the figure.

C. Data Processing

Samples of the band limited version of the channel impulse response were generated by examining the received signal over one sounding signal period of 10 μs. Denote by $s(t)$ the transmitted sounding signal by $r(t)$ the received signal. The relationship between the two is

$$r(t) = s(t) * h(t) + w(t) \tag{1}$$

where $h(t)$ is the unknown channel, $*$ is the convolution operation, and $w(t)$ is the additive thermal noise. The goal is to estimate samples of $h(t)$ from samples of one period of $r(t)$ and $s(t)$. Let T be the sample time where $1/T = 200 \times 10^6$ samples/s and let $r(nT)$ and $s(nT)$ be the n-th sample of $r(t)$ and $s(t)$, respectively. Because there are $N = 2000$ samples in a period, we have $0 \leq n < N$. The required deconvolution operation is performed in the frequency domain. Let $R(e^{j2\pi k/N})$ and $S(e^{j2\pi k/N})$ be the k-th sample of the length-N DFT of $r(t)$ and $s(t)$, respectively, for $0 \leq k < N$. Then the k-th sample of DFT of the channel is

$$\hat{H}(e^{j2\pi k/N}) = \frac{R(e^{j2\pi k/N})}{S(e^{j2\pi k/N})}. \tag{2}$$

Notes:

1) The relationship $R(e^{j2\pi k/N}) = H(e^{j2\pi k/N})S(e^{j2\pi k/N})$ defines the frequency-domain relationship for the *periodic extensions* of $r(nT)$, $h(nT)$, and $s(nT)$. As such, the corresponding time domain relationship $r(nT) = h(nT) * s(nT)$ is thought of as a *circular convolution* [11]. In general, the circular convolution and linear convolution are not equivalent. However, because the transmitted signal is periodic (and one period of the transmitted and received signals are used), the two convolutions are equivalent and (2) gives the desired result.
2) Because the samples $s(nT)$ define a real-valued band-pass signal, the corresponding DFT The division defined in (2) is only performed for the indexes corresponding to the region of support for $S(e^{j2\pi k/N})$. Let this region of support be defined by the indexes $K_1 \leq k \leq K_2$. Given the bandwidth, period, and sample rate, we have $K_2 - K_1 = 500$. Consequently, there are 501 points in the region of support so that $\hat{H}(e^{j2\pi k/N})$ is defined by 501 samples.
3) The discrete-time impulse response $\hat{h}(nT)$ is the inverse DFT of $\hat{H}(e^{j2\pi k/N})$ for $K_1 \leq k \leq K_2$. The sample spacing for $\hat{h}(nT)$ is 5 ns (as determined by the sample rate).

III. Experimental Results

The sampled channel frequency responses measured along the ramp for each pair of transmit and receive antennas are reduced to a sample rate of 200 samples/second, providing a sampling in spatial displacement of the aircraft of approximately 10 samples per wavelength at the center frequency of the transmission. Because of uncertainties regarding the responses of cables and electronics for each transmit and receive antenna, it is necessary to perform calibration on the observed channels before using them to analyze the channel behavior. This calibration involves power normalization and temporal alignment of the channel impulse responses for each antenna pair. In the following, $\hat{H}_{ij}^{(q)}\left(e^{2\pi k/N}\right)$ represents the frequency response from the jth transmit antenna to the ith receive antenna at the qth sample time. The corresponding discrete-time channel impulse response is designated as $\hat{h}_{ij}^{(q)}(nT)$, where we emphasize that nT represents the discretized delay variable.

The power normalization must take into consideration the fact that the receive system uses automatic gain control (AGC) at the intermediate frequency, with the goal of ensuring that each received waveform has the same total received power. As the switches connect different antennas with varying gains, however, the AGC cannot always respond quickly enough to guarantee achievement of this goal. To remove the impacts of the notably different gains associated with the two receive antennas, we scale the responses observed on RX1 and RX2 by different values. Therefore, we compute the total power for the qth channel transfer function from TX3 to RX1 and from TX3 to RX2, denoted respectively as $P_{\mathrm{T},1}^{(q)}$ and $P_{\mathrm{T},2}^{(q)}$. We then normalize the channel transfer functions as

$\hat{H}_{ij}^{(q)} \leftarrow \hat{H}_{ij}^{(q)} / \sqrt{P_{\mathrm{T},i}^{(q)}}$ (functional notation dropped). This preserves the relative scaling between responses for different transmit antennas, since these gains are dictated by antenna placement and not by differences in antenna gain.

With the gains properly normalized, we compute the impulse responses using an inverse DFT. Differences in delays observed in the responses from different transmit antennas are due to different cable lengths to each antenna as well as the different positions of the antennas on the airframe, and these differences are small compared to the delay spreads observed in the multipath channels. In contrast, differences in delays observed in the responses from different receive antennas are significant due to different electronic subsystems and the long cables used to connect these subsystems. Therefore, we align the responses observed on RX1 and RX2 using different temporal shifts. Specifically, for the two channels between TX3 and RX1 and between TX3 and RX2, we define the beginning of the channel impulse response as the first sample at which its magnitude reaches 20% of its peak value, denoted respectively as $n_1^{(q)}$ and $n_2^{(q)}$. Using this definition reduces sensitivity to noise in the waveform and has been found to be robust for accurately detecting the beginning of each response. We then designate sample $n_i^{(q)}$ as zero delay for all three impulse responses observed on RXi.

A. Power Delay Profiles

Given this waveform calibration, we are prepared to examine the multipath delay structure. Specifically, we compute the power delay profile (PDP) of the impulse responses using [12]

$$\mathrm{PDP}_{ij}(nT) = \frac{1}{Q_{\mathrm{m}}} \sum_{q=1}^{Q_{\mathrm{m}}} \left| \hat{h}_{ij}^{(q)}(nT) \right|^2 \tag{3}$$

where Q_{m} is the total number of temporal channel samples over the measurement. This PDP provides an average measure of the power as a function of delay in the multipath channel, and it both gives an indication of the type of fading that might be observed in typical channels and helps to define the complexity of the equalizer that can adequately compensate for the range of multipath delay signatures observed.

Figure 4 plots the PDP waveforms for each transmit-receive antenna pair. Several observations are immediately obvious from these figures. First of all, when compared with the responses observed on RX2, the responses observed on RX1 clearly demonstrate less power arriving in multipaths with long delays. We believe this is due to the fact that long delays are likely to arrive at angles that are notably different from the LOS angle, and since RX1 is more directive than RX2, it does not observe as many of these multipath components. Second, we notice that the components with long delays observed on RX2 appear in a second *cluster* of power (centered at approximately 300 ns in Fig. 4). The reason for this clustering is not entirely clear. However, one possible explanation is that the radiation pattern of RX2 has sidelobes that are higher than those for the pattern of RX1. Since the components with longer delays likely arrive at wide angles, these may be observed on the sidelobes of RX2. Under such circumstances, multipath components with delays around 200 ns might arrive at angles near the first null in the pattern of RX2, which would result in the bi-modal behavior observed.

These PDP plots provide a visual indication of the extent of delay experienced for the observed channels. However, we can further quantify this delay extent using the *average delay spread* for each channel. The average delay spread $\sigma_{\tau,ij}$ for each PDP can be computed using [12]

$$\sigma_{\tau,ij}^2 = \frac{1}{P_{ij}} \sum_n (nT)^2 \ \mathrm{PDP}_{ij}(nT) - \overline{\tau}^2 \tag{4}$$

where

$$P_{ij} = \sum_n \mathrm{PDP}_{ij}(nT) \tag{5}$$

$$\overline{\tau} = \frac{1}{P_{ij}} \sum_n (nT) \ \mathrm{PDP}_{ij}(nT). \tag{6}$$

The delay spread values are included in the PDP plots of Fig. 4. As can be observed, the responses on RX2 have notably larger delay spread values, consistent with the late arrivals of multipath components discussed previously. We also see that for both receive antennas, the delay spread for TX4 is notably larger than that for the other antennas. There are at least two factors that likely contribute to this observation. First, TX4 is on the tail of the helicopter, and the time reference is taken with respect to TX3 on the helicopter belly. As the aircraft attitude changes, the difference in the range to the receive antennas between the belly and tail antennas (TX3 and TX4) can vary by as much as 25 feet in either direction, resulting in about 50 ns of arrival variability for TX4 relative to that for TX3. Second, the position of TX4 makes it more likely for signals to bounce off the lower portion of the main helicopter fuselage and propagate to the receiver, resulting in multipath components with additional delay.

In interpreting these results, it is also helpful to understand that the two receive antennas use different tracking mechanisms. RX1 uses a conical scan to maximize the received signal. Therefore, if the LOS path is obscured, RX1 likely will track on a multipath component, and with the higher gain and narrower beamwidth will be less likely to see other multipath components. In contrast, RX2 tracks by pointing to the GPS coordinates of the aircraft (communicated through a dedicated telemetry link). This means it will point at the aircraft regardless of the quality of the LOS signal, possibly resulting in reduced overall power but richer multipath observations.

B. Diversity Gain

One highly unique feature of the measurements reported in this work is the near-simultaneous transmission from multiple antennas on the aircraft. Because little research exists reporting on the benefits of using spatial diversity on the aircraft, we focus our diversity analysis on the scenario where all three antennas on the aircraft communicate with a single antenna on the ground. To compute the potential diversity gain, we first construct the 3×1 vectors $\mathbf{b}_1^{(q)}(k)$ and $\mathbf{b}_2^{(q)}(k)$, where

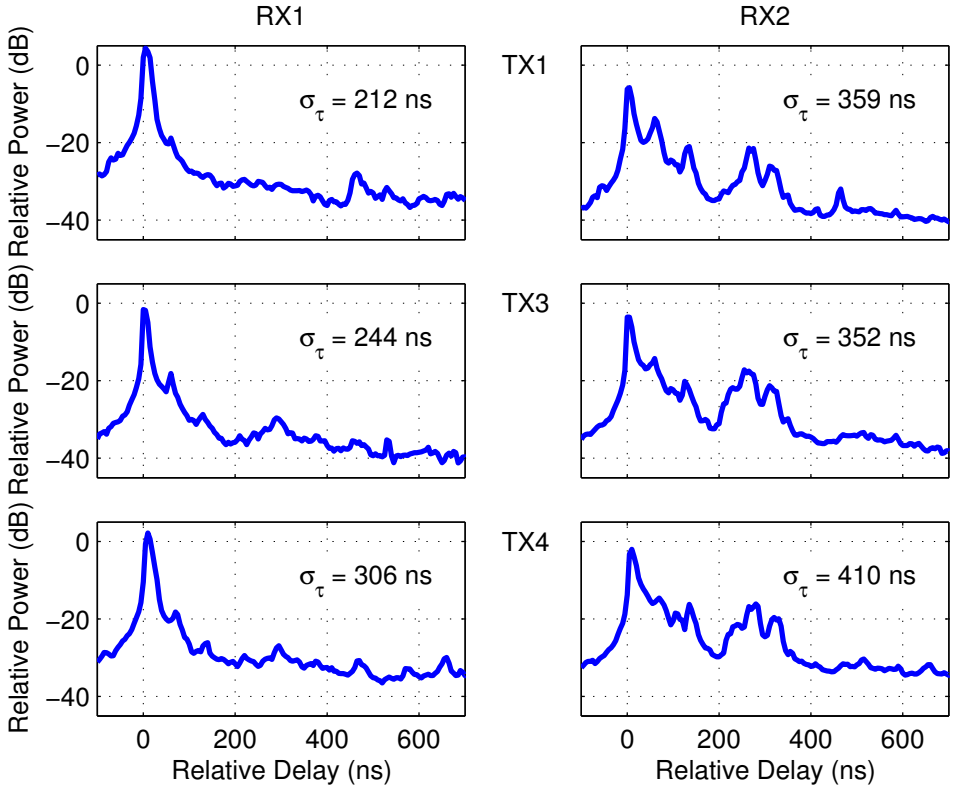

Fig. 4. Power delay profiles observed for each pair of transmit and receive antennas while the helicopter moves along the ramp along with the calculated average delay spreads for each PDP.

the jth element of $\mathbf{b}_i^{(q)}(k)$ is $b_{ij}^{(q)}(k) = \hat{H}_{ij}^{(q)}\left(e^{2\pi k/N}\right)$. From this, we form an estimate of the spatial covariance at the kth frequency, or

$$\mathbf{R}_i^{(Q_0)}(k) = \frac{1}{Q_{\mathrm{w}}} \sum_{q=Q_0}^{Q_0+Q_{\mathrm{w}}-1} \mathbf{b}_i^{(q)}(k)\mathbf{b}_i^{(q)\dagger}(k) \qquad (7)$$

where $Q_0 \leq q < Q_0 + Q_{\mathrm{w}}$ is the time window over which the estimate is computed and $\{\cdot\}^\dagger$ indicates a conjugate transpose operation.

The potential diversity gain observed on each receive antenna can be computed from the eigenvalues of this covariance matrix [13]. To compute this gain, however, we must specify a reference link, with the diversity gain representing the increase in SNR over that of the reference link when diversity signaling is used. Consistent with our developments throughout this section, we use the channel from TX3 to RXi as the reference link for diversity gain computations.

The computations use $Q_{\mathrm{w}} = 50$, which means that the estimation window for the covariance computation represents approximately five wavelengths (or roughly 80 cm) of displacement for the moving helicopter. While this window is somewhat arbitrary, the goal is to use a window over which the multipath structure (delays, angles of departure and arrival) does not change significantly since multipath structural changes can alter the fading statistics. This window should be adequately short to ensure this condition is satisfied. Furthermore, we compute the diversity gain over the entire 50 MHz frequency band in 1 MHz intervals ($1 \leq k \leq 50$).

Figure 5 shows the complementary cumulative distribution function (CCDF) of the achieved diversity gain for each receive antenna assuming the gain for each frequency and spatial sample is treated as a realization of the random variable. Given that RX2 observes richer multipath than RX1, it is not surprising that using diversity on the aircraft generally achieves higher diversity gain for RX2. In considering this result, however, we emphasize that diversity gain represents the improvement in achieved SNR relative to that of a single-antenna link using the reference channel. If, for example, the reference link has very poor SNR, the gain obtained using diversity can be significant. However, higher diversity gain for RX2 does not necessarily mean that the overall SNR observed on RX2 is higher than that observed on RX1, but simply that diversity offers increased relative improvement.

It is also interesting that RX1 is more likely to experience very high diversity gain than RX2. Apparently, there are cases where the reference link to RX1 are very poor (such as when the LOS is highly obscured), and the wide spatial separation of the aircraft antennas leads to significant diversity gains. Because RX2 benefits from additional multipath, in these cases the reference response may be stronger, somewhat reducing the

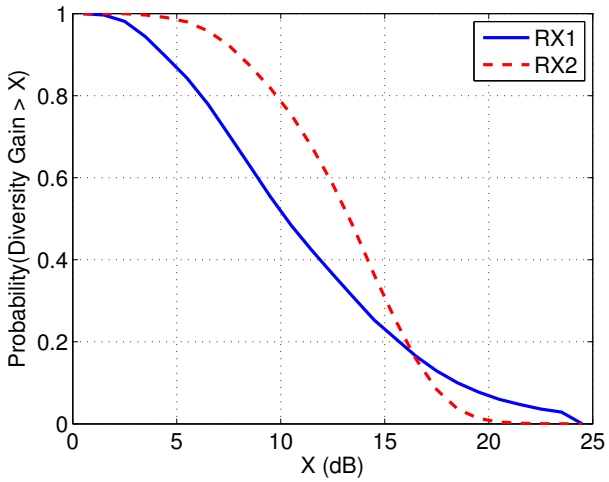

Fig. 5. CCDF of the diversity gain achievable at each receive antenna over all frequencies and spatial channel samples along the ramp.

effectiveness of diversity signaling. It is noteworthy that this high gain occurs at low probability, which is intuitive.

IV. Conclusions

This paper has shown results of measured channels from multiple antenna elements on a helicopter to multiple antennas on the ground in a multipath propagation environment. The channel analysis involves both the delay profile of the multipath channel response as well as the potential diversity gains enabled by properly signaling from multiple aircraft-mounted antennas. The results show that in this environment, delay spreads of the multipath channels vary from about 200 ns to 400 ns, with the longer delay spreads generally resulting when using a receive antenna with lower gain (broader beamwidth) and higher sidelobe levels. Longer delay spreads are also observed with aircraft-mounted antennas whose range to the receiver (relative to the vehicle centroid) can vary significantly with aircraft attitude. The analysis also reveals that on average, diversity signaling from multiple aircraft-mounted antennas can lead to gains in SNR of approximately 13 dB, with the gain notably dependent on the multipath characteristics observed by the ground antenna. These results are useful to those designing channel equalizers and multi-antenna signaling schemes to overcome channel impairments observed in air-to-ground links.

Acknowledgements

The authors acknowledge the hard work and contributions of Mr. Glen Wolf (Delphi Research, Inc., Air Force Flight Test Center) who put the system together; Mr. Michael Mando (U.S. Army Aviation Technical Test Center, Cairns Army Airfield) who made the local arrangements; Mr. Michael Fox (AFTD, Wyle Labs/WESTAR) and Nick Walters (RTC, US Army) who piloted the helicopter.

References

[1] J. Proakis, *Digital Communications*. McGraw-Hill, 2007.

[2] M. Rice, A. Davis, and C. Bettwieser, "A wideband channel model for aeronautical telemetry," *IEEE Transactions on Aerospace and Electronic Systems*, vol. 40, no. 1, pp. 57–69, January 2004.

[3] Q. Lei and M. Rice, "Multipath channel model for over-water aeronautical telemetry," *IEEE Transactions on Aerospace and Electronic Systems*, vol. 45, no. 2, pp. 735 – 742, April 2009.

[4] R. Fan, K. Yao, and D. Whiteman, "Adaptive equalization for OQPSK through a frequency selective fading channel," in *Proceedings of the International Telemetering Conference*, San Diego, CA, October 2000.

[5] Z. Ye, E. Satorius, and T. Jedrey, "Enhancement of advanced range telemetry (ARTM) channels via blind equalization," in *Proceedings of the International Telemetering Conference*, Las Vegas, NV, October 2001.

[6] T. Hill and M. Geoghegan, "A comparison of adaptively equalized PCM/FM, SOQPSK, and multi-h CPM in a multipath channel," in *Proceedings of the International Telemetering Conference*, San Diego, CA, October 2002.

[7] M. Geoghegan, "Experimental results for PCM/FM, Tier I SOQPSK, and Tier II Multi-h CPM with CMA equalization," in *Proceedings of the International Telemetering Conference*, Las Vegas, NV, October 2003.

[8] E. Law, "How well does a blind adaptive CMA equalizer work in a simulated telemetry multipath environment?" in *Proceedings of the International Telemetering Conference*, San Diego, CA, October 2004.

[9] M. Rice and E. Satorius, "A comparison of MMSE and CMA equalization techniques for ARTM tier-1 waveforms," in *Proceedings of the International Telemetering Conference*, San Diego, CA, October 2004.

[10] ——, "Equalization techniques for multipath mitigation in aeronautical telemetry," in *Proceedings of the IEEE Military Communications Conference*, Monterey, CA, November 2004.

[11] A. Oppenheim and A. Willsky, *Signals and Systems*. Prentice Hall, 1996.

[12] R. Vaughan and J. B. Andersen, *Channels, Propagation, and Antennas for Mobile Communications*. London: The Institution of Electrical Engineers, 2003.

[13] O. Nørklit, P. D. Teal, and R. G. Vaughan, "Measurement and evaluation of multi-antenna handsets in indoor mobile communication," *IEEE Trans. Antennas Propagat.*, vol. 49, pp. 429–437, Mar. 2001.